

Quantitative phase analysis (QPA) of the Luserna Stone

GABRIELE VOLA * and MAURIZIO MARCHI

CTG Italcementi Group, Dir. Lab., Via Camozzi 124, 24121, Bergamo, Italy

Submitted, March 2010 - Accepted, July 2010

ABSTRACT - The Luserna Stone (*Pietra di Luserna*) is a leucogranitic orthogneiss, characterized by a micro-Augén texture, with a marked foliation that is mostly associated to a visible lineation: it geologically pertains to the Dora-Maira Massif, and outcrops in a quite large area (approximately 50 km²) of the Cottian Alps, on the border between the Turin and Cuneo provinces (Piemonte, Italy). In this study five samples of granulated rock (1-2 mm) are considered, from three different localities; they are representative of three *facies* (*Massive*, *Splittable* and *Bianchetta*). The mineralogical and petrographic features of this stone, used for many centuries as building material, have been characterised by complementary methods, such as: 1) Quantitative Phase Analysis (QPA) by the Rietveld method using X-ray powder diffraction data (XRPD); 2) mineral modal analysis using optical microscopy (OM) on thin-sections by point-counting a statistical number of grains; 3) scanning electron microscopy equipped with an energy-dispersive spectrometer (SEM-EDS); 4) X-Ray fluorescence spectroscopy (XRF). The proportion of minerals in each sample determined by XRPD and OM are in good agreement between them. The SEM-EDS data combined with mineral proportions determined by XRPD and OM allow to determine bulk chemical compositions of these five samples very close to those obtained by XRF. The decreasing of alkali content determines a linear increase of phyllosilicate and a decreasing of feldspar amounts. These results evidence that complementary methods can efficiently

be used to evaluate undesired constituents in aggregate for concrete, such as phyllosilicates (i.e. micas and chlorites). The combination of XRF and XRPD data allows an accurate and rapid compositional and mineralogical evaluation of the different *facies* of the Luserna Stone.

RIASSUNTO - Il nome “Pietra di Luserna” designa un ortogneiss leucogranitico micro-occhiadino, che affiora in un’area piuttosto ampia (circa 50 km²) delle Alpi Cozie, sul confine tra le province di Cuneo e Torino. Dal punto di vista geologico appartiene al massiccio cristallino Dora-Maira e si caratterizza per una marcata foliazione alla quale è associata una visibile lineazione. In questo studio sono considerati cinque campioni di roccia granulati (1-2 mm), provenienti da tre diverse località, e rappresentativi di tre *facies* (*massiccia*, *fissile* e *bianchetta*). Questi campioni sono stati caratterizzati mediante i seguenti metodi tra loro complementari: 1) analisi quantitativa delle fasi (QPA), mediante metodo Rietveld, su spettri di diffrazione ai raggi X per polvere (XRPD); 2) analisi modale in microscopia ottica (OM) su sezione sottile, mediante conteggio per punti su un numero significativo di granuli; 3) microscopia elettronica a scansione equipaggiata con spettrometro a dispersione di energia (SEM-EDS); 4) analisi spettroscopica in fluorescenza ai raggi X (XRF). Le proporzioni delle fasi mineralogiche determinate mediante XRPD e OM sono tra loro in buono accordo. Le analisi mediante SEM-EDS combinate con le proporzioni delle fasi

* Corresponding author, E-mail: g.vola@itcgr.net

mineralogiche determinate mediante XRPD e OM consentono di calcolare la composizione chimica elementare, che risulta essere prossima a quella determinata mediante XRF. La diminuzione nel contenuto di alcali determina un incremento lineare dei fillosilicati e una riduzione del contenuto di feldspati. Tali risultati evidenziano che la complementarità dei metodi può essere efficientemente usata per valutare i costituenti indesiderati negli aggregati per calcestruzzo, come i fillosilicati (miche e cloriti). La combinazione delle analisi XRF e XRPD consente di determinare in modo accurato e rapido la composizione mineralogica delle tre differenti *facies* di Pietra di Luserna.

KEY WORDS: *Luserna Stone; concrete aggregates; quantitative phase analysis; Rietveld method;*

phyllosilicates content.

INTRODUCTION

The Luserna Stone (*Pietra di Luserna*) outcrops in the Luserna-Infernotto basin (Cottian Alps, Piedmont) on the border between the Turin and Cuneo provinces. It pertains to the Dora-Maira Massif (Sandrone *et al.*, 1993) that represents a part of the ancient European margin annexed to the Cottian Alps during Alpine orogenesis. The Luserna Stone (Sandrone *et al.*, 2000; 2001) is a Lower Permian orthogneiss, resulting from the metamorphism of a leucogranitic rock (Compagnoni *et al.*, 1982-83).

From a petrographic point of view, the Luserna

TABLE I
Physical-mechanical characterization of the Luserna Stone.

Determination	Reference	U.M.	<i>Massive Facies</i>	<i>Splittable Facies</i>	Category
Compressive strength	Regione Piemonte (2000)	MPa	128	-	-
Flexural strength	Regione Piemonte (2000)	MPa	21.3	24.3	-
Impact strength	Regione Piemonte (2000)	J	8.0	8.8	-
Knoop micro hardness	Regione Piemonte (2000)	MPa	4269	4486	-
Water absorption	Regione Piemonte (2000)	%	0.29	0.31	-
Fineness Coefficient	Vola <i>et al.</i> , 2008	%	0.95	0.96	-
Shape index	Vola <i>et al.</i> , 2008	%	20	22	SI ₄₀
Flakiness index	Vola <i>et al.</i> , 2008	%	19	21	FI ₃₅
Los Angeles Coefficient	Vola <i>et al.</i> , 2008	%	29	27	LA ₃₀
Micro-Deval Coefficient	Vola <i>et al.</i> , 2008	%	10	7	M _{DE} 10
Bulk Mass	Vola <i>et al.</i> , 2008	g/cm ³	2.65	2.63	-
Total Porosity (MIP)	Vola <i>et al.</i> , 2008	%	1.2	1.3	-
BET/N ₂ Specific Surface Area	Vola <i>et al.</i> , 2008	m ² /g	0.4	0.3	-

Stone is characterized by a micro *Augen* texture, with a grey-greenish or locally pale blue colour. In the field, the Luserna Stone has a sub-horizontal attitude, with a marked fine-grained foliation that is mostly associated with visible lineation. The mineralogical composition includes (in order of abundance): quartz (30–45%), albite (15–25%), K-feldspar (10–25%), and phengite (10–20%), whereas subordinated (less than 5%) phases are: biotite, chlorite, zoisite and/or clinozoisite/epidote. Common accessory phases are ore minerals, titanite, apatite, zircon, tourmaline, locally are present also carbonates, rare axinite and frequent fluorite (Sandrone *et al.*, 2001; Sandrone *et al.*, 2004).

Textural and structural rock features allow to distinguish three varieties of the Luserna Stone gneiss: *Splittable facies*, *Massive facies* and a more rare white variety called *Bianchetta facies* (Sandrone *et al.*, 2001). The physical and mechanical properties of the Luserna Stone are excellent, showing very good compressive, flexural and impact strength and low water absorption (Regione Piemonte, 2000). The physical-mechanical characterization of aggregates from quarry “waste” was already performed by Vola *et al.* (2008), and reported in TABLE 1.

The Luserna Stone exploitation and processing is significant in the Italian natural stone business since the second half of the 19th century. Recently the quarried amounts are approximately 391,000 m³ per year, but 71,500 m³ of them are mined but not used (D’Amato *et al.*, 2005); thus, about 18 % of the quarried amount per year is normally destined to dumps. Moreover, materials already dumped in the past are estimated to be about 4,000,000 m³. According to the current legislation, these quarry “wastes” are by-products considerable as a raw materials for further processing, and until now partially used for hydro-geological stabilization (blocks for river embankments and retaining walls) or as aggregates for road sub-bases and

railway ballasts (Sandrone *et al.*, 1989; Sandrone *et al.*, 2000; Lovera *et al.*, 2001; Fornaro, 2003; Dino and Fornaro, 2005). Moreover, these materials were also used as aggregates for civil works during the Winter Olympic Games of Torino 2006 (435,000 m³), and for the construction of the highway Torino-Pinerolo (250,000 m³, D’Amato *et al.*, 2005).

Recent studies and tests done by CTG Italcementi Group with the support of Calcestruzzi Spa subsidiary, deal with a technical-economic assessment for the re-use of these stone by-products. To further constrain the possibility of using and/or improving the quality control of the Luserna Stone dumps as possible aggregate for concrete, we investigated the mineralogical and petrographic features of it by complementary analytical methods. We especially focused on the evaluation of phyllosilicates content which is considered a critical factor for casting the concrete (Vola *et al.*, 2008; Vola and Marchi, 2009; Vola *et al.*, 2010; Vola *et al.*, in press).

ROCK SAMPLING AND ANALYTICAL METHODS

Five representative specimens from the Luserna Stone basin have been sampled in this study. The first two specimens represent the *Massive facies* (*Seccarezze district*), the third and fourth the *Splittable facies* (*Ciaffalco and Bricco Volti districts*) and the last one the *Bianchetta facies* (*Ciaffalco district*). The label, petrography and provenance of these representative three *facies* are reported in TABLE 2.

X-ray powder diffraction (XRPD)

XRPD data were obtained on powdered samples with a Bruker D8-Advance X-Ray powder Diffractometer operating with a parafocusing geometry; it is equipped with CuK α radiation, two sets of soller slits and a LynxEye™ PSD Detector. All XRPD spectra were collected between 5-70° of 2 θ with a step

TABLE 2
Sample labels, petrography, facies and provenance.

Label	Lithotype	Facies	Quarry Locations (districts)
2006-4031	Orthogneiss	Massive	Seccarezze
2007-6909	Orthogneiss	Massive	Seccarezze
2006-4032	Orthogneiss	Splittable	Ciaffalco
2007-6908	Orthogneiss	Splittable	Bricco Volti
2006-4033	Orthogneiss	Bianchetta	Ciaffalco

TABLE 3
Minerals identified in the Luserna Stone samples by XRPD.

Label	Facies	Main Phases	Subordinate Phases
2006-4031	Massive	Qtz + Ab + Mc	Phg + Bt + Clc + Ttn
2007-6909	Massive	Qtz + Ab + Mc	Phg + Bt + Clc + Czo
2006-4032	Splittable	Qtz + Ab + Mc + Phg	Clc + Bt + Ttn
2007-6908	Splittable	Qtz + Ab + Mc + Phg	Clc + Bt
2006-4033	Bianchetta	Qtz + Ab + Phg	Mc + Czo + Ttn

Mineral (according to Siivola and Schmid, 2007): Qtz: quartz; Ab: albite; Mc: microcline; Phg: phengite; Bt: biotite; Czo: clinozoisite; Clc : Fe-clinocllore; and Ttn: titanite.

of 0.02° per second. The collected XRPD data were treated to obtain Quantitative Phase Analysis (QPA) using the Rietveld method (Rietveld, 1969; Young, 1993). After the identification of mineral phases (TABLE 3), crystallographic structural models for the Rietveld refinement were selected from literature data (TABLE 4). All refinements were carried out using the GSAS-EXPGUI software package (Larson and Von Dreele, 2000; Toby, 2001). The background was firstly fitted, using a Chebishev function with six coefficients. Then, peak profiles were modelled for each phase using a pseudo-Voigt function with one Gaussian and one Lorentzian coefficient. Successively, the zero offset, cell parameters and phase fractions were refined. Phases with contents lower than 0.5 % by weight were not considered in the final cycles of Rietveld refinements. A preferred

orientation correction using the March model revised by Dollase was applied for the (101) and (100) peaks for quartz, (001) and (010) for albite and microcline and (001) for phengites, biotite and clinocllore.

Optical Microscopy (OM)

Luserna Stone by-products firstly were crushed and then sieved, to obtain 1-2 mm fine-aggregate fractions for petrographic examination. Thin sections were then prepared using these obtained fine-aggregate glued in araldite for each sample (TABLE 2). Optical Microscopy observations were carried out using an Olympus BX 51 petrographic microscope equipped with a point-counter apparatus, on a statistical number of grains (Sims and Nixon, 2003). This protocol allows to obtain statistical orientation of a wide number of grains in order to obtain a reliable and accurate

TABLE 4
Crystallographic structural models used for Rietveld refinements.

Mineral phase	Powder Diffraction Files database	References
Quartz	79634-ICSD	Glinnemann <i>et al.</i> (1992)
Albite low	26248-ICSD	Ribbe <i>et al.</i> (1969)
Microcline int.	9542-ICSD	Bailey (1969)
Phengite 2M1	87844-ICSD	Pavese <i>et al.</i> (1999)
Phengite 3T	1100016 data	Pavese <i>et al.</i> (1997)
Clinochlore	84262-ICSD	Smyth <i>et al.</i> (1997)
Clinoisite	9001799 data	Comodi and Zanazzi (1997)
Biotite	9002301 data	Brigatti <i>et al.</i> (2000)
Titanite	9000509 data	Taylor and Brown (1976)

determination of mineral fractions.

SEM-EDS and XRF

Textural and micro-chemical data on thin sections were carried out with a Leo Scanning Electron Microscope (SEM), equipped with a Sirius Energy Dispersive Spectrometer (EDS). Major element chemical analysis was performed with a PANalytical CubiX X-Ray Fluorescence (XRF) spectrometer using the following conditions (M.H.T. = 50 kV, M.A.C. = 4 mA).

RESULTS

X-ray powder diffraction (XRPD)

QPA results carried out by the Rietveld method and relative agreement factors are reported in TABLE 5. The mineralogy of the Luserna Stone quantitatively determined in this study by XRPD data are in agreement with previous investigations (Pagliani, 1954; Vialon 1966; Compagnoni *et al.*, 1982-83; Sandrone *et al.*, 2001).

The QPA data show that quartz is the main phase for all the three *facies* of the Luserna Stone (between 39.9 and 48.1 % by weight); the second most important phase is albite (between 25.5 and 33.6 % by weight), whereas microcline is the third abundant phase in the *Massive* and the *Splittable facies*; microcline amount is instead

around 2 % by weight in the *Bianchetta facies* (TABLE 5). The low amount of microcline in the *Bianchetta facies* is balanced by higher contents of quartz and albite (TABLE 5). For phengite, two different structure models, 2M1 and 3T, were considered. These two polytypes can coexist (Ivaldi *et al.*, 2001), but they cannot be easily distinguished by XRPD. Thereby, we performed different refinements alternating these two models or using both of them. Albeit differences among these three possibilities are very low, the final and adopted solution was chosen according to the best agreement factor attained (TABLE 5). The refinement of the *Bianchetta facies* XRPD pattern shows the best fitting using both polytypes (2M1 and 3T), whereas for the *Massive facies* only the polytype 2M1 has been considered. Rietveld refinements of the *Splittable* samples were performed using the polytype 3T for the specimen 2006-4032 and the polytype 2M1 for the specimen 2007-6908. The amount of phengite (2M1 or 3T), increases from the *Massive* to *Splittable facies* samples and reaches the highest value in the sample of the *Bianchetta facies* (with both polytypes 2M1 and 3T). Biotite is invariably less than 3 % by weight for both *Massive* and the *Splittable facies* and has been not detected in the *Bianchetta* sample (TABLE 5). Fe-clinocllore (chamosite) is quite low in both the *Massive* and *Splittable*

TABLE 5
Quantitative Phase Analysis determined by the Rietveld method (XRD-QPA).

label	2006-4031	2007-6909	2006-4032	2007-6908	2006-4033
Facies	<i>Massive</i>	<i>Massive</i>	<i>Splittable</i>	<i>Splittable</i>	<i>Bianchetta</i>
Cycles	1150	1439	974	782	1149
χ^2	3.97	4.106	4.295	4.117	4.325
R_{wp}	8.90	9.44	9.22	9.21	9.22
Mineral	Phase fraction (% by weight)				
Qtz	41.1 (0)	41.9 (0)	39.9 (0)	45.5 (0)	48.1 (0)
Ab	29.3 (1)	25.5 (1)	28.2 (2)	27.3 (2)	33.6 (2)
Mc	21.3 (2)	22.8 (2)	20.7 (2)	15.3 (2)	1.8 (2)
Phg_2M1	3.5 (2)	5.3 (2)	0.0	7.6 (2)	7.8 (2)
Phg_3T	0.0	0.0	7.5 (2)	0.0	6.4 (2)
Clc	1.4 (1)	2.6 (1)	1.2 (1)	1.7 (2)	0.0
Czo	0.0	1.1 (1)	0.0	0.0	1.6 (2)
Bt	2.6 (1)	0.8 (0)	1.5 (1)	2.6 (2)	0.0
Ttn	0.9 (0)	0.0	0.9 (1)	0.0	0.8 (1)
Feldspars	50.9	48.3	48.9	42.6	35.5
Phyllosilicates	7.5	8.6	10.2	11.9	14.2
Total	100	100	100	100	100

Footnotes: $^a R_p = \sum |y_{obs} - y_{calc}| / \sum y_{obs}$; $^b R_{wp} = [\sum w(y_{obs} - y_{calc})^2 / \sum w y_{obs}^2]^{1/2}$; $\chi = \sum w(y_{obs} - y_{calc})^2 / (N_{obs} - N_{var})$

facies samples and it is absent in the *Bianchetta* one, whereas clinozoisite is an accessory phase in the *Massive* and *Bianchetta* samples and is lacking in the *Splittable* one (TABLE 5). Finally, titanite is absent or close to 1 % by weight in the three samples.

Optical Microscopy (OM)

The optical and textural characteristics for each recognized mineral phase are reported in this section. Quartz (Qtz) is fine-grained and occur as anhedral porphyroblasts of 200-300 μm ; usually forms ribbon quartz or layers associated with feldspar eyes often surrounded by parallel flakes of mica. Very fine grains are commonly located into the microcline pressure-shadows. Albite (Ab) occurs as sub-millimetre to millimetre-size prismatic porphyroblasts (\varnothing_{Max} 1-2 mm), generally with a fresher and clearer appearance than quartz, often squeezed into elliptic or lens-shaped forms; it shows

multiple and “flame” twinning, with inclusions of phengite and rarely of apatite. Microcline (Mc) is present as millimetre-size porphyroclasts with irregular rims, usually presenting fractures along cleavage planes and rotation of fragments; Mc shows Carlsbad simple twinning and soft vanishing “tartan” twinning (albite and pericline) and commonly hosts inclusions of apatite and sericite (as incipient weathering product). Phengite (Phg) has yellowish to pale green pleochroic lepidoblasts, with moderate relief and elongation in the same direction of cleavage, straight extinction and mottling in extinction position; this mineral phase is normally associated with zoisite and/or clinozoisite and commonly distributed into layers of mica alternating with quartz-rich and feldspar-rich layers; phengite mainly controls the stone cleavage and split workability. Biotite (Bt) occurs as pleochroic lepidoblasts with colour zoning of the core-margin type (pale green to

green-brown core, pale yellow margin); biotite has a tabular habit, a moderate relief and is often associated with clinocllore and phengite. Clinocllore (Clc) is pleochroic in shades of light-green lepidoblasts with moderate relief; it has a lamellar habit, one set of micaceous cleavage, straight extinction and anomalous violet or blue interference colours typical of Fe-rich varieties (chamosite). Clinozoisite (Czo) is present as brownish shagreened porphyroblasts with very low pleochroism and moderate relief; Czo shows ultra blue and rarely first-order pale yellow interference colours and it can be mainly distinguished from zoisite for the inclined extinction, optically negative and very high 2V. Zoisite (Zo) occurs as porphyroblasts with high relief, colourless and good cleavage, straight extinction, very low birefringence with anomalous interference colours; it is possible to distinguish Czo from Zo by the optically positive sign with a moderate 2V. Titanite (Ttn) has

yellow to brown pleochroic porphyroblasts with a lozenge habit; Biotite (Bt) has a poor cleavage, an inclined extinction, a very high relief and birefringence. Apatite (Ap) is colourless and occurs with rounded habit porphyroblasts; it shows a poor cleavage, a high relief and a low birefringence. Calcite (Cal) is colourless, with a moderate relief and birefringence; it has a yellowish-cream interference colours and is more frequently found in the *Bianchetta facies* associated to quartz and feldspars. Zircon (Zrn) is non-pleochroic and occurs as rounded or tetragonal habit porphyroblasts, with pale brown colour, poor cleavage, straight extinction, very high relief and birefringence; zircon is also hosted in phengite flakes.

The quantity (% by volume) of mineral phases by OM for each of the five samples is reported in TABLE 6. Similarly to XRPD data, quartz and albite are by far the most abundant phases for all the five analyzed samples. Microcline is the third

TABLE 6
Quantitative Phase Analysis determined by Optical Microscopy (OM) observations on thin sections.

label	2006-4031	2008-6909	2006-4032	2008-6908	2006-4033
Facies	<i>Massive</i>	<i>Massive</i>	<i>Splittable</i>	<i>Splittable</i>	<i>Bianchetta</i>
Mineral	Phase fraction (% by volume)				
Qtz	39.9	40.9	45.2	42.1	51.2
Ab	28.7	27.6	24.1	24.8	27.1
Mc	23.8	21.4	20.7	18.5	4.4
Phg	4.8	5.5	4.7	11.9	13.2
Clc	1.1	2.3	2.3	0.4	0.1
Czo/Zo	0.4	0.8	0.5	1.0	2.8
Bt	0.8	1.2	1.8	0.6	0.0
Ttn	0.2	0.1	0.0	0.1	0.0
Ap	0.3	0.1	0.7	0.5	0.8
Cal	0.0	0.0	0.0	0.0	0.1
Zrn	0.1	0.0	0.1	0.1	0.4
Feldspars	52.4	49.0	44.8	43.3	31.4
Phyllosilicates	6.7	9.1	8.7	13.0	13.3
Total	100	100	100	100	100
Number of analysed points	900	902	1021	941	965

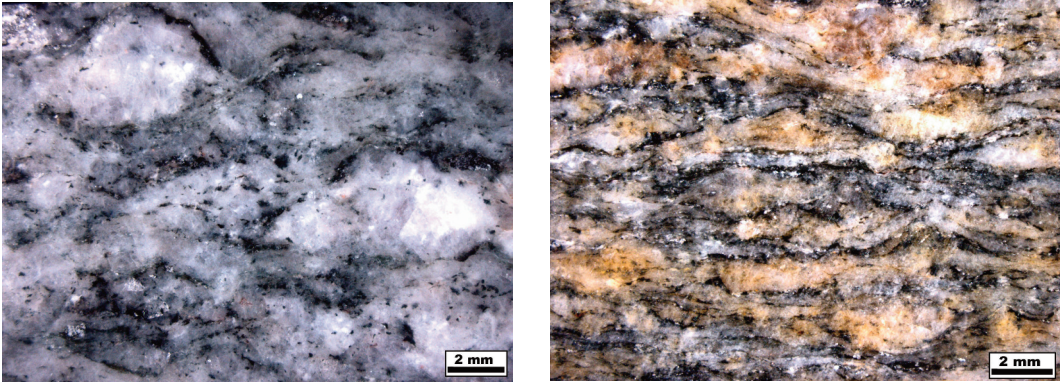


Fig. 1 - Stereoscopic micrographs of Luserna Stone: A: *Massive facies*; B: *Splittable facies*.

most abundant mineral for the *Massive* and *Splittable facies*; for the *Bianchetta* sample, phengite (2M1 and 3T) is more abundant than microcline (TABLE 6). Biotite is lacking in the *Bianchetta facies* and between 0.6 and 1.8 % by volume in the other two *facies* (TABLE 6). Clinocllore amount is very low for the *Bianchetta* sample and between 0.4 and 2.3 % by volume for the other two *facies*, whereas clinzoisite and/or zoisite are lower than 1 % by volume in the *Massive* and *Splittable facies* but is 2.8 % by volume in the *Bianchetta* sample (TABLE 6).

The mesoscopic textural features of the

Massive and *Splittable facies* are shown in Fig. 1; in agreement with Sandrone et al. (2001), the micro *Augen* gneiss of the *Splittable facies* shows thin deformed feldspar eyes and regular schistosity planes with centimetre spacing, whereas the *Massive facies* has not so elongated and closer feldspar eyes resulting in a lower schistosity. The microscopic textural features of the *Bianchetta* sample are reported in Fig. 2. The textural features of this *facies* is intermediate between the *Massive* and *Splittable* ones; in agreement with XRPD data, the main difference of the *Bianchetta facies* with respect the other two ones is that phengite is higher than

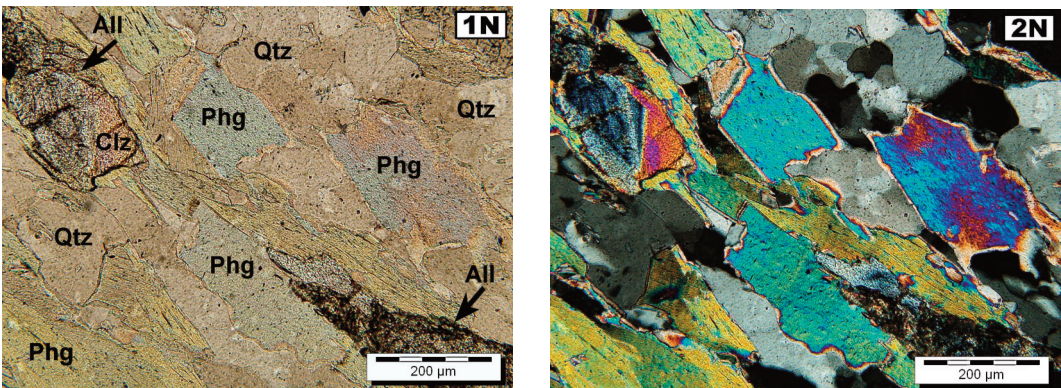


Fig. 2 - Luserna Stone OM micrographs show the characteristic mineralogical layering composed of phengite (Phg), quartz (Qtz), clinozoisite (Czo) and allanite (All). *Bianchetta facies*.

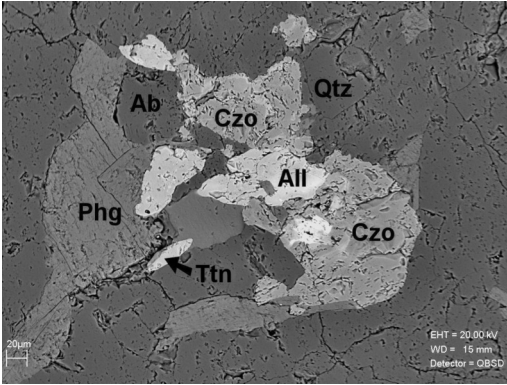


Fig. 3 - BSE image shows epidote group (Zo/Czo margin, All core), phengite (Phg) and titanite (Ttn). The dark field surrounding is composed of quartz (Qtz) and albite (Ab). Specimen 2006-4031, *Massive facies*.

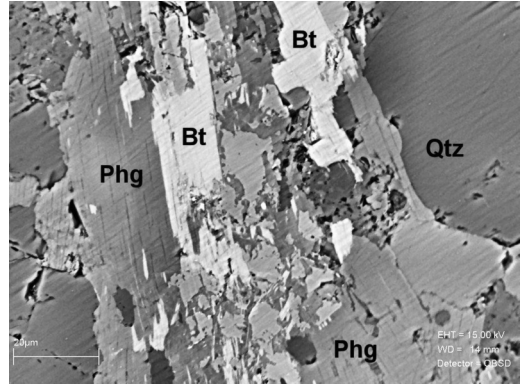


Fig. 4 - BSE image shows the characteristic intergrowth of darker phengite (Phg) laminas with brighter biotite (Bt) laminas. Specimen 2007-6908, *Splittable facies*.

microcline.

SEM-EDS and XRF

The five thin sections have been observed also

by SEM to corroborate the OM observations and to measure the micro-chemical (semi-quantitative) compositions by EDS of each mineral phase. Representative BSE-images of

TABLE 7
Average SEM-EDS microanalyses of the sample 2006-4031 (*Massive facies*).

Det. (Wt.%)	Ab	Mc	Phg	Clc	Czo	Bt
SiO ₂	71.0	65.2	50.7	25.3	39.6	35.5
TiO ₂	0.0	0.0	0.1	0.0	0.0	1.3
Al ₂ O ₃	20.9	19.3	30.4	20.3	23.4	16.3
Fe ₂ O ₃	0.0	0.0	6.5	50.3	15.5	34.0
Mn ₂ O ₃	0.0	0.0	0.1	0.6	0.0	0.3
MgO	0.0	0.0	1.2	3.4	0.0	3.3
CaO	0.0	0.0	0.0	0.0	20.7	0.0
SrO	0.0	0.0	0.0	0.0	0.0	0.0
Na ₂ O	8.1	0.0	0.0	0.1	0.0	0.0
K ₂ O	0.0	15.5	10.9	0.0	0.0	9.3
P ₂ O ₅	0.0	0.0	0.0	0.0	0.0	0.0
SO ₃	0.0	0.0	0.0	0.0	0.0	0.0
Ce ₂ O ₃	0.0	0.0	0.0	0.0	0.6	0.0
ThO ₂	0.0	0.0	0.0	0.0	0.2	0.0
Tot	100	100	100	100	100	100

TABLE 8
Average SEM-EDS microanalyses of the sample 2007-6909 (Massive facies).

Det (Wt.%)	Ab	Mc	Phg	Clc	Czo	Bt
SiO ₂	70.6	65.4	53.1	26.3	39.7	35.9
TiO ₂	0.0	0.0	0.3	0.0	0.0	1.5
Al ₂ O ₃	20.5	19.2	26.8	21.1	26.0	18.0
Fe ₂ O ₃	0.0	0.0	7.5	48.1	11.7	32.0
Mn ₂ O ₃	0.0	0.0	0.0	0.5	0.0	0.2
MgO	0.0	0.0	1.5	3.7	0.0	3.1
CaO	0.0	0.0	0.2	0.0	22.6	0.0
SrO	0.0	0.0	0.0	0.0	0.0	0.0
Na ₂ O	8.7	0.3	0.0	0.1	0.0	0.0
K ₂ O	0.1	15.2	10.6	0.2	0.0	9.4
SO ₃	0.0	0.0	0.0	0.0	0.0	0.0
P ₂ O ₅	0.0	0.0	0.0	0.0	0.0	0.0
Tot	100	100	100	100	100	100

TABLE 9
Average SEM-EDS microanalyses of the sample 2006-4032 (Splittable facies).

Det. (Wt.%)	Ab	Mc	Phg	Clc	Czo	Bt
SiO ₂	71.4	65.1	55.3	25.3	36.9	34.0
TiO ₂	0.0	0.0	0.3	0.0	0.0	1.7
Al ₂ O ₃	21.3	19.2	26.5	18.3	22.2	16.2
Fe ₂ O ₃	0.0	0.0	4.8	50.4	16.0	34.3
Mn ₂ O ₃	0.0	0.0	0.0	0.0	0.0	0.0
MgO	0.0	0.0	2.6	5.5	0.0	3.3
CaO	0.0	0.0	0.0	0.0	24.8	0.0
SrO	0.0	0.0	0.0	0.0	0.0	0.0
Na ₂ O	7.2	0.0	0.0	0.0	0.0	0.0
K ₂ O	0.0	15.7	10.6	0.5	0.0	10.4
P ₂ O ₅	0.0	0.0	0.0	0.0	0.0	0.0
SO ₃	0.0	0.0	0.0	0.0	0.0	0.0
Tot.	100	100	100	100	100	100

TABLE 10
Average SEM-EDS microanalyses of the sample 2007-6908 (Splittable facies).

Det. (Wt.%)	Ab	Mc	Phg	Clc	Czo	Bt
SiO ₂	70.7	65.4	53.2	30.6	39.9	36.5
TiO ₂	0.0	0.0	0.0	0.0	0.0	1.0
Al ₂ O ₃	20.8	19.3	27.5	22.5	28.1	20.1
Fe ₂ O ₃	0.0	0.0	7.3	41.5	9.2	30.6
Mn ₂ O ₃	0.0	0.0	0.0	0.0	0.0	0.1
MgO	0.0	0.0	1.2	3.7	0.0	3.0
CaO	0.0	0.0	0.0	0.0	22.8	0.0
SrO	0.0	0.0	0.0	0.0	0.0	0.0
Na ₂ O	8.2	0.5	0.0	0.2	0.0	0.0
K ₂ O	0.4	14.9	10.8	1.5	0.0	8.7
P ₂ O ₅	0.0	0.0	0.0	0.0	0.0	0.0
SO ₃	0.0	0.0	0.0	0.0	0.0	0.0
Tot.	100	100	100	100	100	100

TABLE 11
Average SEM-EDS microanalyses of the sample 2006-4033 (Bianchetta facies).

Det. (Wt.%)	Ab	Mc	Phg	Czo	Ttn
SiO ₂	72.2	64.5	50.1	39.6	32.7
TiO ₂	0.0	0.0	0.0	0.0	32.4
Al ₂ O ₃	20.4	18.7	31.6	29.1	5.6
Fe ₂ O ₃	0.0	0.0	5.3	6.4	0.0
Mn ₂ O ₃	0.0	0.0	0.0	0.0	0.0
CaO	0.0	0.0	0.0	24.5	29.3
MgO	0.0	0.2	0.9	0.0	0.0
Na ₂ O	7.4	0.3	0.0	0.0	0.0
K ₂ O	0.0	16.2	12.1	0.0	0.0
SrO	0.0	0.0	0.0	0.0	0.0
P ₂ O ₅	0.0	0.0	0.0	0.0	0.0
SO ₃	0.0	0.0	0.0	0.0	0.0
Ce ₂ O ₃	0.0	0.0	0.0	0.5	0.0
Tot.	100	100	100	100	100

TABLE 12
Representative SEM-EDS microanalyses of accessory phases.

Det. (Wt.%)	All (1)	Ap (2)	Ilm (3)	Zrn (4)	Fl (2)
SiO ₂	32.1	0.0	6.7	29.0	0.0
TiO ₂	0.1	0.0	50.4	0.0	0.0
Al ₂ O ₃	16.1	0.0	0.0	0.0	0.0
Fe ₂ O ₃	7.2	0.0	38.3	0.0	0.0
Mn ₂ O ₃	0.0	0.0	4.6	0.0	0.0
CaO	12.4	42.4	0.0	0.0	63.8
P ₂ O ₅	0.0	55.2	0.0	0.0	0.0
HfO ₂	0.0	0.0	0.0	1.4	0.0
ZrO ₂	0.0	0.0	0.0	69.6	0.0
YO ₃	14.7	0.0	0.0	0.0	0.0
Ce ₂ O ₃	12.0	0.0	0.0	0.0	0.0
La ₂ O ₃	4.5	0.0	0.0	0.0	0.0
ThO ₂	1.0	0.0	0.0	0.0	0.0
F-	0.0	2.4	0.0	0.0	36.2
Tot.	100	100	100	100	100

Symbols legend: 1 = average from specimen 2006-4031; 2 = average from all the specimens; 3 = average from specimen 2006-4032; 4 = average from specimens 2006-4031, 4032, and 2007-6909.

mineral assemblages and relative textural and structural features are reported in Figures 3 and 4. The average composition of albite (Ab), microcline (Mc), phengite (Phg), Fe-clinocllore (Clc), clinozoisite (Czo) and biotite (Bt) for each investigated sample are reported in TABLES 7, 8, 9, 10 and 11.

On the basis of these semi-quantitative data it is possible to constrain the general compositional features of these minerals. Plagioclase crystals in each sample are close to a pure albite with very low amount of K. By contrast, the amount of Na in microcline crystals is limited (TABLES 7, 8, 9, 10 and 11). Micas are both enriched in K, with very low amounts of Na and Ca. Muscovites are very close to the phengite ideal composition, while the biotites ranges over the iron-rich members of the phlogopite-annite series. Chlorites in all samples are brunsvigites (chamosite series) on the basis of Fe/(Fe+Mg) ratio (see chlorites diagram in Hey, 1954)

(TABLES 7, 8, 9, 10 and 11). Discontinuous zoning and intergrowths of epidotes of different composition have been frequently observed, with margins of clinozoisite-type and cores of allanites-type. The composition of margins varies between moderate (e.g. *Bianchetta facies*) and iron-rich members (e.g. *Massive* and *Splittable facies*) of the clinozoisite-epidote series. The appreciable amount of rare earth elements in the cores (e.g. Y, Ce, La and Th) represents the transition towards allanite series (TABLE 12). Microanalyses of the remaining accessory phases allanites (All), apatite (Ap), ilmenite (Ilm), zircon (Zrn), and fluorite (Fl) are reported in TABLE 12.

Bulk chemical compositions (oxide % by weight) determined by XRF spectroscopy for each sample are reported in TABLE 13. The SiO₂ plus Al₂O₃ amount for each sample is close to 90 % by weight of these five samples; the *Bianchetta facies* shows the highest amount of

TABLE 13

Bulk chemical composition of the five samples of the Luserna Stone measured by XRF and calculated by SEM-EDS coupled with QPA by XRPD and by OM.

label	2006-4031			2007-6909			2006-4032			2007-6908			2006-4033		
facies	<i>Massive</i>			<i>Massive</i>			<i>Splittable</i>			<i>Splittable</i>			<i>Bianchetta</i>		
oxide (% by weight)	XRD	OM	XRF	XRD	OM	XRF	XRD	OM	XRF	XRD	OM	XRF	XRD	OM	XRF
SiO ₂	79.1	79.0	75.9	79.1	78.7	77.6	78.8	79.9	77.6	80.3	78.8	75.6	81.5	81.4	78.9
TiO ₂	0.3	0.1	0.1	0.0	0.1	0.1	0.3	0.0	0.1	0.0	0.0	0.1	0.3	0.0	0.1
Al ₂ O ₃	12.0	12.5	12.2	12.0	12.2	11.2	12.5	11.2	11.8	11.6	12.5	12.6	12.2	11.3	12.2
Fe ₂ O ₃	1.8	1.2	1.1	2.0	2.0	1.4	1.5	2.1	1.2	2.1	1.3	1.6	0.8	0.9	0.9
Mn ₂ O ₃	0.0	0.0	0.0	0.0	0.0	0.0	0.0	0.0	0.0	0.0	0.0	0.1	0.0	0.0	0.0
MgO	0.2	0.1	0.1	0.2	0.2	0.1	0.3	0.3	0.2	0.2	0.2	0.2	0.1	0.1	0.1
CaO	0.3	0.3	0.3	0.3	0.3	1.1	0.3	0.4	0.2	0.0	0.5	0.7	0.6	1.1	0.4
SrO	0.0	0.0	0.1	0.0	0.0	0.0	0.0	0.0	0.0	0.0	0.0	0.0	0.0	0.0	0.1
Na ₂ O	2.4	2.3	3.5	2.3	2.5	3.0	2.0	1.7	3.2	2.3	2.1	2.9	2.5	2.0	3.6
K ₂ O	3.9	4.3	5.6	4.1	4.0	4.9	4.2	3.9	4.6	3.4	4.2	5.0	2.0	2.3	2.2
P ₂ O ₅	0.0	0.2	0.0	0.0	0.1	0.1	0.0	0.4	0.0	0.0	0.3	0.2	0.0	0.4	0.0
SO ₃	0.0	0.0	0.2	0.0	0.0	0.1	0.0	0.0	0.2	0.0	0.0	0.1	0.0	0.0	0.2
L.o.i.	n.d.	n.d.	0.6	n.d.	n.d.	0.3	n.d.	n.d.	0.7	n.d.	n.d.	0.8	n.d.	n.d.	1.0
Tot.	100	100	99.7	100	99.9	99.9	100	100	99.8	100	99.9	99.8	100	99.6	99.6

SiO₂ and the lowest of Fe₂O₃ (TABLE 13). MgO is invariably low for each sample, whereas CaO is lesser than 1 % by weight, except for sample 2007-6909 (TABLE 13). The samples of the *Massive* and *Splittable facies* have alkali contents relatively high, ranging approximately between 7 and 9 % by weight; conversely, alkali are significantly lower for the *Bianchetta* sample (TABLE 13).

DISCUSSION AND CONCLUSIONS

Quantitative phase analyses (QPA) obtained by XRPD (% by weight) and OM (% by volume) are in good agreement between them for each of the investigated sample (TABLES 5 and 6). The phase proportion determined by OM (% by volume) has been also recalculated according to the density of minerals taking in account their semi-quantitative chemical compositions obtained by SEM-EDS (TABLES 7-12). The QPA differences in % by weight between XRPD and OM are low.

The five Luserna Stone samples considered here (TABLE 2), show that quartz is by far the most abundant mineral for all samples and the amount of quartz in the *Bianchetta* sample accounts to about half of this rock (TABLES 5 and 6). The content of feldspars (Ab + Mc) is higher than that of phyllosilicates (Phg + Clc + Bt) in each analysed sample. However, Mc (and feldspars) is markedly low and phengitic micas high in the *Bianchetta* sample in comparison with the other four specimens; the low amount of Mc in the *Bianchetta facies* is mainly balanced by increasing amounts of quartz and phyllosilicate phases (TABLES 5 and 6). Quartz and feldspars (Ab + Mc) amounts are generally higher in the *Massive* specimens than in the *Splittable* ones; conversely, the amount of phyllosilicates (Phg + Bt + Clc) is higher in specimens of *Splittable facies* than in the *Massive* ones, according to their split workability. The amount of phengite in the *Bianchetta* sample determined in this study is the largest ever reported for the Luserna Stone;

previous investigations considered the *Splittable facies* - in which the amount of phengite is around 7 % by weight (by XRPD) - the richest in micas (Alciati, 1999).

The reliability of QPA has been further checked comparing the bulk chemical composition of each sample determined by XRF with that calculated by SEM-EDS micro-chemical coupled with XRPD and OM QPA determinations. The obtained results are reported in TABLE 13. Both the re-calculated analyses (XRPD and OM) don't consider the hydroxyls contribution from the hydrated phases; this determines a light overestimation of other elements, especially Si. However, differences of these complementary bulk chemical compositions are also close among them (TABLE 13). These low differences definitively state that both XRPD and OM methods allow to obtain accurate mineral proportions of any *facies* of the Luserna Stone.

OM analyses on thin sections allow to determine textural and structural features of the Luserna rocks, re-crystallization and weathering processes suffered by these stones and to identify all the accessory phases not detectable by XRPD. On the other hand, the QPA by OM is extremely

time consuming due to the large number of counts required for a representative statistic. The main limitation using XRPD data is that the identification of accessory phases can be difficult or even impossible; on the other hand, the preferred orientation of some minerals (especially feldspars and phyllosilicates) and the adopted structural models (TABLE 4) of minerals do not significantly limit the accuracy of QPA by XRPD since important solid solutions in minerals have been not detected by SEM-EDS (TABLES 7-12). Taking in account the accuracy and relative rapidity of QPA by the XRPD method, it is then possible to use Rietveld refinement for routinely characterisation of the Luserna Stone.

In conclusion, compositional and mineralogical characterisation of the Luserna Stone can be carried out with a good accuracy by XRF and XRPD complementary analyses, especially for the determination of phyllosilicates. These methods can be also corroborated between them as evidenced in Fig. 5; the increasing of alkali (mainly K) content is linearly and inversely dependent on the amount of phyllosilicates, whereas as Na and K increase feldspars also increase (Fig. 5). The content of phyllosilicates in aggregates is critical, especially when exceeding 12% by weight; in turn, an accurate determination of the phyllosilicate fraction is extremely important because workability of fresh pastes and strength in hardened concretes are reduced (Dewar, 1963; De and Jain, 1977; Smith and Collis, 1993; Wakizaka *et al.*, 2005; Vola *et al.*, 2008; Vola and Marchi, 2009). For the Luserna Stone, the *Massive facies* appears to be the most useful for aggregates due to its lower phyllosilicates content, but unfortunately “wastes” deriving from all the *facies* are dumped together. However, preliminary analyses on aggregates of different size-classes (0-3, 2-5, 3-8, 5-15, 15-30 mm) obtained by means of an industrial crushing test on 110 tons of the Luserna Stone “wastes” from the Galiverga dump area, gave encouraging

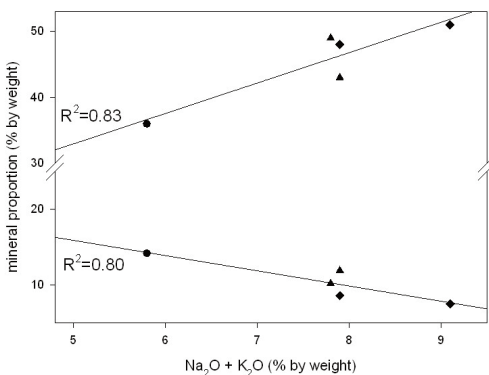


Fig. 5 - Relationship between alkali (by XRF) and phyllosilicate and feldspar (by XRPD) contents for *Bianchetta* (circle), *Massive* (diamond) and *Splittable* (triangle) *facies*.

results, because the average content of phyllosilicates is 9.2%, ranging between 8.0 to 11.5 % (Vola *et al.*, 2010).

The determination of phyllosilicate fractions by XRPD and XRF methods, checked by OM and SEM-EDS complementary analyses, for the Luserna Stone can be applied to other gneissic stone by-products (Vola *et al.*, in press).

ACKNOWLEDGEMENTS

The Authors are grateful to Prof. R. Sandrone (Politecnico di Torino), Dr. A. Cavallo (Università degli Studi Milano-Bicocca), and Dr. G. Iezzi (Università degli Studi 'G. d'Annunzio' di Chieti-Pescara) for the constructive critical review of the manuscript. Authors are also particularly grateful to Mr. B. Zanga and Dr. M. Segata (CTG Bergamo) for XRD data, and to Dr. E. Borgarello (CTG R&D Dept.) for supporting this research activity.

REFERENCES

- ALCIATI L. (1999) - *Studio geo-petrografico della pietra di Luserna. Caratteri tecnico-economici del bacino estrattivo ed esame dei processi di lavorazione del materiale*. Tesi di laurea inedita, Università Torino, Corso di laurea in Scienze Geologiche, 173 p.
- BAILEY S.W. (1969) - *Refinement of an intermediate microcline structure*. *Am. Mineral.*, **54**, 1540-1545.
- BRIGATTI M.F., FRIGIERI P., GHEZZO C. and POPPI L. (2000) - *Crystal chemistry of Al-rich biotites coexisting with muscovites in peraluminous granites*. *Am. Mineral.*, **85**, 436-448.
- COMODI P. and ZANAZZI P.F. (1997) - *The pressure behavior of clinozoisite and zoisite: an X-ray diffraction study*. *Am. Mineral.*, **82**, 61-68.
- COMPAGNONI R., CRISCI G.M. and SANDRONE R. (1982-83) - *Caratterizzazione chimica e petrografica degli "gneiss di Luserna" (Massiccio cristallino Dora-Maira, Alpi Occidentali)*. *Rend. Soc. It. Min. Petr.*, **38**, 498.
- D'AMATO A., DINO G.A., FORNARO M., LOVERA E. and VIGLIERO L. (2005) - *Gli sfridi di cava per realizzare le grandi opere pubbliche. L'esperienza della Regione Piemonte per il riutilizzo degli sfridi di pietre ornamentali nelle grandi opere pubbliche*. Quarry and Construction, 7, luglio 2005. Pei Parma, 61-77.
- DE P.L. and JAIN V.K. (1977) - *Use of micaceous sand for concrete and mortar*. *Indian Concrete Journal*, **51**, 56-58.
- DEWAR J.D. (1963) - *Effect of mica in the fine aggregate on the water requirement and strength of concrete*. Cement and Concrete Association, Technical Report, TRA/370, april 1963, 4p.
- DINO G.A. and FORNARO M. (2005) - *L'utilizzo integrale delle risorse lapidee negli aspetti estrattivi, di lavorazione e di recupero ambientale dei siti*. *Giorn. Geol. Appl.*, **2**, 320-327.
- FORNARO M. (Ed.) (2003) - *Ricerca concernente il riutilizzo alternativo degli sfridi di cava*. Relazione sulla prima fase della ricerca (2002/2003). Contratto di consulenza tecnico-scientifica tra la Regione Piemonte e l'Università degli Studi di Torino, Dipartimento di Scienze della Terra, Torino, dicembre 2003, 56 p.
- GLINNEMANN J., KING H.E. jr, SCHULZ H., HAHN Th., LA PLACA S.J. and DACOL F. (1992) - *Crystal structures of the low-temperature quartz-type phases of SiO₂ and GeO₂ at elevated pressure*. *Z. Kristallogr.*, **198**, 177-212.
- HEY M. H. (1954) - *A new review of chlorites*. *Mineral. Mag.*, **30**, 277-292.
- IVALDI G., FERRARIS G., CURETTI N. and COMPAGNONI R. (2001) - *Coexisting 3T and 2M1 polytypes of phengite from Cima Pal (Val Savenca, western Alps): Chemical and polytypic zoning and structural characterization*. *Eur. J. Mineral.*, **13**, 1025-1034.
- LARSON A.C. and VON DREELE R.B. (2000) - *General Structure Analysis System (GSAS)*. Los Alamos National Laboratory Report LAUR, 86-748.
- LOVERA E., RADICCI M. T. and SACERDOTE R. (2001) - *La coltivazione della Pietra di Luserna nelle cave del polo estrattivo di Seccarezze: tecnologie e produttività*. *Atti Sem. Int. "Le pietre ornamentali della montagna europea"*, Luserna S. Giovanni - Torre Pellice (To), 10-12 giugno 2001, 277-286.
- PAGLIANI G. (1954) - *Studio petrografico del gneiss di Luserna (Alpi Cozie)*. *Ist. Lombardo Sci. Lett.*, **87**, 493-514.
- PAVESE A., FERRARIS G., PISCHEDDA V. and IBBERSON R. (1999) - *Tetrahedral order in phengite 2M₁ upon heating, from powder neutron diffraction, and thermodynamic consequences*. *Eur. J. Mineral.*, **11**, 309-320.
- PAVESE A., FERRARIS G., PRENCIPE M. and IBBERSON R.

- (1997) - *Cation site ordering in phengite 3T from the Dora-Maira Massif (Western Alps); a variable-temperature neutron powder diffraction study*. Eur. J. Mineral., **9**, 1183-1190.
- REGIONE PIEMONTE (2000) - *Pietre ornamentali del Piemonte. Piedmont's ornamental stone*. Redaprint, Verona, 127 p.
- RIBBE P.H., MEGAW H.D., TAYLOR W.H., FERGUSON R.B. and TRAILL R.J. (1969) - *The albite structures*. Acta Crystallogr., **B25**, 1503-1518.
- RIETVELD H.M. (1969) - *A profile refinement for nuclear and magnetic structures*. J. Appl. Crystallogr., **2**, 65-71.
- SANDRONE R., FORNARO M. and MASTROMAURO N. (1989) - *Valorizzazione degli scarti e sviluppo nel bacino della "Pietra di Luserna"*. Conv. Int. "Situazione e prospettive dell'industria lapidea", Cagliari, 3-5 aprile 1989, 343-350.
- SANDRONE R., CADOPPI P., SACCHI R. and VIALON P. (1993) - *The Dora-Maira Massif*. In: VON RAUMER J.F. and NEUBAUER F. (Eds.) - *Pre-Mesozoic geology in the Alps*. Springer, Berlin, 317-325.
- SANDRONE R., ALCIATI L., DE ROSSI A., FIORA L. and RADICCI M.T. (2000) - *Estrazione, lavorazione e impieghi della Pietra di Luserna*. Proc. "Quarry-Laboratory-Monument" Int. Congr., Pavia 2000, **2**, 41-49.
- SANDRONE R., ALCIATI L., DE ROSSI A., FIORA L., RADICCI M.T. and RE P. (2001) - *La Pietra di Luserna*. In: ALCIATI L. and SANDRONE R. (Eds.) - *Guida alle escursioni*. Atti Sem. Int. "Le Pietre Ornamentali della Montagna Europea", Luserna San Giovanni - Torre Pellice (To), 10-12 giugno 2001, 347-355.
- SANDRONE R., COLOMBO A., FIORA L., FORNARO M., LOVERA E., TUNESI A. and CAVALLO A. (2004) - *Contemporary natural stones from the Italian Western Alps (Piedmont and Aosta Valley Regions)*. Period. Mineral., **73** (special issue 3), 211-226.
- SHIVOLA J. and SCHMID R. (2007) - *Recommendations by the IUGS Subcommittee on the Systematics of Metamorphic Rocks. List of Mineral Abbreviations*. Web version 01.02.07. (http://www.bgs.ac.uk/scmr/docs/papers/paper_12.pdf) IUGS Commission on the Systematics in Petrology.
- SIMS I. and NIXON P. (Eds.) (2003) - *RILEM recommended test method AAR-1: Detection of potential alkali-reactivity of aggregates - Petrographic method*. Mater. Struct., **36**, 480-496.
- SMITH M.R. and COLLIS L. (Eds.) (1993) - *Aggregates-Sand, Gravel and Crushed Rock Aggregates for Construction Purposes*, Engineering Geology Special Publication, **9**, Geological Society, London.
- SMYTH J.R., DYAR M.D., MAY H.M., BRICKER O.P. and ACKER J.G. (1997) - *Crystal structure refinement and Moessbauer spectroscopy of an ordered, triclinic clinocllore*. Clays Clay Miner., **45**, 544-550.
- TAYLOR M. and BROWN G.E. (1976) - *High-temperature structural study of the P21/a ↔ A2/a phase transition in synthetic titanite, CaTiSiO₅*, Am. Mineral., **61**, 435-447.
- TOBY B.H. (2001) - *EXPGUI, a graphical user interface for GSAS*. J. Appl. Crystallogr., **34**, 210-213.
- VIALON P. (1966) - *Etude géologique du Massif Cristallin Dora-Maira (Alpes Cottiennes internes - Italie)*. Trav. Lab. Géol. Grenoble, Mém., **4**, 293.
- VOLA G., SANDRONE R., ZICHELLA L. and ALLEVI S. (2008) - *Caratterizzazione degli scarti di coltivazione di Pietra di Luserna per la produzione di aggregati da calcestruzzo*. Rend. online Soc. Geol. It., **3**, 782-783.
- VOLA G. and MARCHI M. (2009) - *Mineralogical and petrographic quantitative analyses of a recycled aggregate from quarry wastes. The Luserna Stone Case-Study*. In: MIDDENDORF B., JUST A., KLEIN D., GLAUBITT A. and SIMON J. (Eds.) - Proc. 12th Euroseminar on Microscopy Applied to Building Materials (EMABM), Dortmund, 15th-19th September 2009, 270-282.
- VOLA G., LOVERA E., TEZZA R. and PIAZZA E. (2010) - *Re-use of by-products of the "Luserna Stone" for construction materials: technologies, environmental sustainability and economic feasibility*. In: NAIK T.R. & CANPOLAT F. and CLAISSE P. & GANJIAN E. (Eds.) - Honor Session Proc. 2nd Int. Conf. on Sustainable Construction Materials and Technologies (SCMT), Ancona, June 28-30, 2010, 43-58.
- VOLA G., HERVE S., REGNAUD L., ALLEVI S., ALFANI R. and VICHOT A. (in press) - *The Effect of Phyllosilicates in By-Products Aggregates on Rheological Behaviour of Cement-Based formulations*. In Proc. XIII Int. Congr. on Chemistry of Cement (ICCC), Madrid, July 3-8, 2011.
- YOUNG R.A. (Eds.) (1993) - *The Rietveld Method*. International Union of Crystallography (IUCr), Monograph on crystallography, **5**, Oxford Science Publications, 300p.